

# The Role of Nuclear Coulomb Attraction in Nonsequential Double Ionization of Argon Atom

Qing Liao, Yueming Zhou, and Peixiang Lu<sup>†</sup>

Wuhan National Laboratory for Optoelectronics, Huazhong University of Science and  
Technology, Wuhan 430074, P. R. China

<sup>†</sup>Corresponding author: [lupeixiang@mail.hust.edu.cn](mailto:lupeixiang@mail.hust.edu.cn)

**Abstract:** The role of nucleus in strong-field nonsequential double ionization of Ar atoms is investigated using three-dimensional classical ensembles. By adjusting the nuclear Coulomb potential, we can excellently reproduce the experimental correlated electron and ion momentum spectra with laser intensities above the recollision threshold [Phys. Rev. Lett. 93, 263001 (2004)] and below the recollision threshold [Phys. Rev. Lett. 101, 053001 (2008)] quantitatively. Analysis reveals the detailed electronic dynamics when the nuclear Coulomb attraction plays a key role in the recollision process of nonsequential double ionization of Ar atoms. Comparison between our results for Ar and those for He shows that atom species have a strong influence on nonsequential double ionization.

© 2021 Optical Society of America

**OCIS codes:** (020.4180) Multiphoton processes; (260.3230) Ionization; (270.6620) Strong-field processes. quadrants.

---

## References and links

1. A. l’Huillier, L. A. Lompre, G. Mainfray, and C. Manus, “Multiply charged ions induced by multiphoton absorption in rare gases at  $0.53 \mu\text{m}$ ,” Phys. Rev. A **27**, 2503–2512 (1983).
2. B. Walker, B. Sheehy, L. F. DiMauro, P. Agostini, K. J. Schafer, and K. C. Kulander, “Precision measurement of strong field double ionization of helium,” Phys. Rev. Lett. **73**, 1227–1230 (1994).
3. Th. Weber, H. Giessen, M. Weckenbrock, G. Urbasch, A. Staudte, L. Spielberger, O. Jagutzki, V. Mergel, M. Vollmer, and R. Dörner, Correlated electron emission in multiphoton double ionization, Nature **405**, 658–661 (2000).
4. Th. Weber, M. Weckenbrock, A. Staudte, L. Spielberger, O. Jagutzki, V. Mergel, F. Afaneh, G. Urbasch, M. Vollmer, H. Giessen, and R. Dörner, “Recoil-Ion momentum distributions for single and double ionization of helium in strong laser fields,” Phys. Rev. Lett. **84**, 443–446 (2000).
5. X. Liu, H. Rottke, E. Eremina, W. Sandner, E. Goulielmakis, K. O. Keeffe, M. Lezius, F. Krausz, F. Lindner, M. G. Schaätzle, G. G. Paulus, and H. Walther, “Nonsequential double ionization at the single-optical-cycle limit,” Phys. Rev. Lett. **93**, 263001 (2004).
6. M. Weckenbrock, D. Zeidler, A. Staudte, Th. Weber, M. Schöffler, M. Meckel, S. Kammer, M. Smolarski, O. Jagutzki, V. R. Bhardwaj, D. M. Rayner, D. M. Villeneuve, P. B. Corkum, and R. Dörner, “Fully differential rates for femtosecond multiphoton double ionization of neon,” Phys. Rev. Lett. **92**, 213002 (2004).
7. Q. Liao, P. Lu, Q. Zhang, Z. Yang, and X. Wang, “Double ionization of  $\text{HeH}^+$  molecules in intense laser fields,” Opt. Express **16**, 17070–17075 (2008).
8. A. Becker and F. H. M. Faisal, “Interpretation of momentum distribution of recoil ions from laser induced non-sequential double ionization,” Phys. Rev. Lett. **84**, 3546–3549 (2000).
9. J. S. Parker, B. J. S. Doherty, K. T. Taylor, K. D. Schultz, C. I. Blaga, and L. F. DiMauro, “High-energy cutoff in the spectrum of strong-field nonsequential double ionization,” Phys. Rev. Lett. **96**, 133001 (2000).
10. Yunquan Liu, S. Tschuch, A. Rudenko, M. Drr, M. Siegel, U. Morgner, R. Moshhammer, and J. Ullrich, “Strong-field double ionization of Ar below the recollision threshold,” Phys. Rev. Lett. **101**, 053001 (2008).

11. C. Figueira de Morisson Faria, H. Schomerus, X. Liu, and W. Becker, "Electron-electron dynamics in laser-induced nonsequential double ionization," *Phys. Rev. A* **69**, 043405 (2004).
12. R. Panfili, J. H. Eberly and S. L. Haan, "Comparing classical and quantum dynamics of strong-field double ionization," *Opt. Express* **8**, 431–435 (2001).
13. S. L. Haan, L. Breen, A. Karim, and J. H. Eberly, "Variable Time lag and backward ejection in full-dimensional analysis of strong-field double ionization," *Phys. Rev. Lett.* **97**, 103008 (2006).
14. Yueming Zhou, Qing Liao, and Peixiang Lu, "Mechanism for high-energy electrons in nonsequential double ionization below the recollision-excitation threshold," *Phys. Rev. A* **80**, 023412 (2009).
15. R. Moshhammer, B. Feuerstein, W. Schmitt, A. Dorn, C. D. Schröter, and J. Ullrich, "Momentum distributions of  $\text{Ne}^{m+}$  ions created by an intense ultrashort laser pulse," *Phys. Rev. Lett.* **84**, 447–450 (2000).
16. P. B. Corkum, "Plasma perspective on strong field multiphoton ionization," *Phys. Rev. Lett.* **71**, 1994–1997 (1993).
17. B. Feuerstein, R. Moshhammer, D. Fischer, A. Dorn, C. D. Schröter, J. Deipenwisch, J. R. Crespo Lopez-Urrutia, C. Höhr, P. Neumayer, J. Ullrich, H. Rottke, C. Trump, M. Wittmann, G. Korn, and W. Sandner, "Separation of recollision mechanisms in nonsequential strong field double ionization of Ar: The role of excitation tunneling," *Phys. Rev. Lett.* **87**, 043003 (2001).
18. A. Staude, C. Ruiz, M. Schöffler, S. Schössler, D. Zeidler, Th. Weber, M. Meckel, D. M. Villeneuve, P. B. Corkum, A. Becker, and R. Dörner, "Binary and recoil collisions in strong field double ionization of helium," *Phys. Rev. Lett.* **99**, 263002 (2007).
19. A. Rudenko, V. L. B. de Jesus, Th. Ergler, K. Zrost, B. Feuerstein, C. D. Schröter, R. Moshhammer, and J. Ullrich, "Correlated two-electron momentum spectra for strong-field nonsequential double ionization of He at 800 nm," *Phys. Rev. Lett.* **99**, 263003 (2007).
20. S. L. Haan, J. S. Van Dyke, and Z. S. Smith, "Recollision excitation, electron correlation, and the production of high-momentum electrons in double ionization," *Phys. Rev. Lett.* **101**, 113001 (2008).
21. J. Chen and C. H. Nam, "Ion momentum distributions for He single and double ionization in strong laser fields," *Phys. Rev. A* **66**, 053415 (2002).
22. P. J. Ho, R. Panfili, S. L. Haan, and J. H. Eberly, "Nonsequential double ionization as a completely classical photoelectric effect," *Phys. Rev. Lett.* **94**, 093002 (2005).
23. Y. Zhou, Q. Liao, Q. Zhang, W. Hong, P. Lu, "Controlling nonsequential double ionization via two-color few-cycle pulses," *Opt. Express* **18**, 632–638 (2010).
24. M. Kieß, T. Löffler, M. D. Thomson, R. Dörner, H. Gimpel, K. Zrost, T. Ergler, R. Moshhammer, U. Morgner, J. Ullrich, and H. G. Roskos, Determination of the carrier-envelope phase of few-cycle laser pulses with terahertz-emission spectroscopy, *Nature Phys.* **2**, 327–331 (2006).
25. Q. Liao, P. X. Lu, Q. B. Zhang, W. Y. Hong, and Z. Y. Yang, Phase-dependent nonsequential double ionization by few-cycle laser pulses, *J. Phys. B* **41**, 125601 (2008).
26. S.L. Haan, L. Breen, A. Karim, and J.H. Eberly, "Recollision dynamics and time delay in strong-field double ionization," *Opt. Express* **15**, 767–778 (2007).
27. G. G. Paulus, F. Lindner, H. Walther, A. Baltuška, E. Goulielmakis, M. Lezius, and F. Krausz, "Measurement of the phase of few-cycle laser pulses," *Phys. Rev. Lett.* **91**, 253004 (2003).
28. Qing Liao, Peixiang Lu, Pengfei Lan, Zhenyu Yang, and Yuhua Li, "Method to precisely measure the phase of few-cycle laser pulses," *Opt. Express* **16**, 6455–6460 (2008).

---

## 1. Introduction

Nonsequential double ionization (NSDI) of atoms and molecules has provided a profound understanding of laser-matter interaction and electron correlation [1-7]. In order to explore the physical mechanism of NSDI, a series of experimental and theoretical studies [2-6, 8-15] have been performed. The rescattering model [16] is now widely accepted to be the basic mechanism of NSDI at near infrared (NIR) wavelengths. In the rescattering picture, one electron firstly escapes from the atom near the peak of the electric field. After changing its direction, the laser field drives the electron back to the parent ion and then causes the ionization of the bound electron through the inelastic recollision. According to this model, if the second electron is ionized directly through the recollision, the process is called (e, 2e) ionization, i.e. recollision-ionization (RCI), whereas if the second electron is excited through the recollision with subsequent field-ionization by the laser field, the process is called recollision excitation with subsequent ionization (RESI) [17]. Based on this inelastic rescattering mechanism, at low laser intensities, RESI mechanism dominates NSDI and the longitudinal momentum distributions of the doubly charged ions exhibits a single peak structure near zero momentum [3]. While at high laser in-

tensities, RCI mechanism dominates NSDI and the longitudinal momentum distributions of the doubly charged ions will exhibit a double-peak structure at nonzero momenta [5, 17].

It has been shown that the microscopic dynamics of NSDI is dependent on the atom species because of the different atom structures [15, 17]. Recent experimental studies [18, 19] showed that the nuclear Coulomb attraction plays a significant role in forming the finger-like pattern of the correlated electron momentum distributions from strong-field double ionization of helium. The important role of nuclear Coulomb attraction was firstly demonstrated in [20] by the three-dimensional (3D) classical ensembles model [13]. In order to quantitatively reproduce the experimental results of NSDI for different atoms and predict new experimental phenomena, employing the proper nuclear Coulomb potentials for different atoms is of vital importance.

In this paper, we report the calculation results of correlated momentum spectra from NSDI of Ar atoms by intense laser pulses with intensities above and below the recollision threshold using the three-dimensional (3D) classical ensembles [13, 20]. In this model, the nuclear Coulomb potential is described by soft-core Coulomb potential. By adjusting the nuclear Coulomb potential to a proper form, we can excellently reproduce two experimental results [5, 10]. Back analysis reveals that the nuclear Coulomb attraction has a strong influence on the microscopic dynamics in the recollision process. By comparing the nuclear Coulomb potential of He atoms, we can infer that the inner-shell electrons also have a significant influence on NSDI of Ar atoms.

## 2. The classical Ensemble Model

The 3D classical ensembles has been described in detail in [13, 20]. This model has achieved great successes in studying the NSDI process [13, 14, 20, 23]. This classical model discards all aspects of quantum mechanics. In this model, the first ionization occurs over a laser-suppressed barrier [20], not through tunneling, which is retained within a semi-classical model [21]. However, the classical model is adequate to generate very strong two-electron correlation in NSDI [22]. Many recollision details [13, 14, 20, 22, 26] are revealed by this model. By back-tracing the trajectories, recollision mechanisms can be classified into RCI mechanism if the delay time between closest recollision and double ionization is less than 0.25 laser cycle and RESI mechanism if larger than 0.25 laser cycle [26]. This classification of recollision mechanisms is consistent with that in [17]. RCI trajectories give distributions of doubly charged ions peaked at nonzero momenta and RESI trajectories give a distribution of ions peaked at zero momentum. Another classification of trajectories: nonzero and zero momenta trajectories in [22], are in accordance with RCI and RESI trajectories respectively. In our simulations, a large ensemble containing one or two millions classical electron pairs is used. The evolution of the system is determined by the classical equation of motion (Atomic units are used throughout the paper unless otherwise stated):  $d^2\vec{r}_i/dt^2 = -\vec{E}(t) - \vec{\nabla}[V_{ne}(\vec{r}_i) + V_{ee}(\vec{r}_1, \vec{r}_2)]$ , where the subscript  $i$  is denotes the two different electrons and  $\vec{E}(t)$  is the linearly polarized electric field. The nucleus-electron and the electron-electron interaction are represented by 3D soft-Coulomb potential  $V_{ne} = -2/\sqrt{r_i^2 + a^2}$  and  $V_{ee} = 1/\sqrt{(\vec{r}_1 - \vec{r}_2)^2 + b^2}$ , respectively. To obtain the initial value, the ensemble is populated starting from a classically allowed position for the argon ground-state energy of -1.59 a.u. The available kinetic energy is distributed between the two electrons randomly in momentum space. Each electron is given a radial velocity only, with sign randomly selected [13]. Then the electrons are allowed to evolve a sufficient long time(100 a.u.) in the absence of the laser field to obtain stable position and momentum distributions. To avoid autoionization and ensure stability in three dimensions, the nuclear soft-core parameter  $a$  is set to be larger than 1.26 a.u. In this paper, we set to  $a = 1.5$  a.u. Then, in order to explore the influence of nuclear Coulomb potential on the process of recollision, we can decrease the value of  $a$  after first ionization. To conserve energy we offset the decrease in the potential energy of each electron with a kinetic boost for its radial motion [20]. The soft-core parameter  $b$

is set to be 0.05 a.u. throughout the whole process. The nucleus remains fixed at the origin at all times. After the laser pulse is turned off, if both electrons have positive energy, we define double ionization.

### 3. Results and Discussions

Firstly, we show the calculation results of NSDI of Ar atoms by intense laser pulses with an intensity well above the recollision threshold. The laser parameters are employed as the same as in the experiment of Ref.[5]. The laser pulse is a linear polarized few-cycle pulse. Its electric field is  $\vec{E}(t) = \vec{e}_x E_0 \sin^2(\pi t/Nt) \cos[\omega(t - NT/2) + \phi]$ , where  $\vec{e}_x$  is the polarization vector.  $E_0$ ,  $\omega$ ,  $T$  and  $\phi$  are the amplitude, frequency, period and carrier-envelope phase (CEP), respectively. The wavelength  $\lambda=760$  nm, the carrier frequency  $\omega=0.06$  a.u., the intensity  $I=3.5 \times 10^{14}$  W/cm<sup>2</sup> and period of laser cycle  $T=2\pi/\omega$ . The pulse contains five laser cycles, where the full-width at half-maximum is about 5 fs.

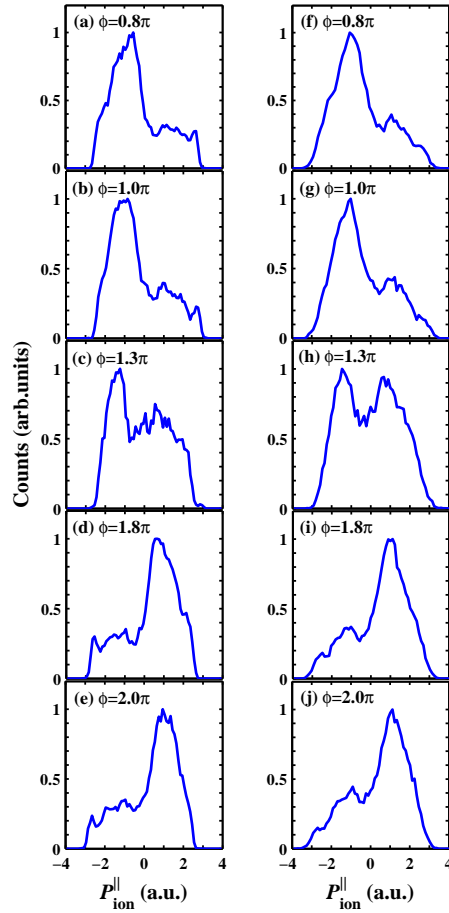


Fig. 1. (color online). Momentum spectra of the Ar<sup>2+</sup> ions for different CEPs  $\phi = 0.8\pi$  (a, f),  $1.0\pi$  (b, g),  $1.3\pi$  (c, h),  $1.8\pi$  (d, i) and  $2.0\pi$  (e, j), respectively. According to the laser parameters,  $\pm 4\sqrt{U_p} = \pm 3.33$  a.u. The soft-core parameters  $a=1.5$  a.u. for Figs. 1(a)-1(e) and  $a = 1.0$  a.u. for Figs. 1(f)-1(j) after first ionization.

The recoil momentum of the Ar<sup>2+</sup> ion is the sum of the two electron momenta with a reversed

direction [22], i.e.  $P_{ion}^{\parallel} = -(P_{e1}^{\parallel} + P_{e2}^{\parallel})$ , because the photon momentum is negligible. The final-state longitudinal momentum spectra of the doubly charged ions as a function of the CEP is shown in Fig. 1, where the values of the CEP  $\phi = 0.8\pi$ (a, f),  $1.0\pi$ (b, g),  $1.3\pi$ (c, h),  $1.8\pi$ (d, i) and  $2.0\pi$ (e, j), respectively. In Figs. 1(a)-1(e), the soft-core parameter  $a$  keeps unchanged (1.5 a.u.) in the whole double ionization process. Though the ion momentum distributions are sensitive to the CEP of the pulse, they are different from the experimental results (Figs. 2(a)-2(e) of Ref. [5]). When decreasing the soft-core parameter  $a$  after first ionization to enhance the role of nuclear Coulomb attraction in recollision process, we find that the calculation results are in good agreement with the experimental results only for  $a = 1$  a.u., as shown in Figs. 1(f)-1(j). The ion longitudinal momentum spectra are prominent asymmetric. A change for the asymmetry appears with the center of gravity of the ion momentum distributions shifting from negative to positive as the CEP increases from  $0.8\pi$  to  $2\pi$ . While the CEP  $\phi = 1.3\pi$ , a double-hump structure with maxima of nearly equal yields appears. As the CEP  $\phi = 0.8\pi$  (or  $1.8\pi$ ), the asymmetry reaches the maximum. Compared with Figs. 1(a)-1(e), the ion momentum spectra of Figs. 1(f)-1(j) exhibit three prominent changes. Firstly, the range of the momentum spectra becomes broader and equal to the range of  $[-4\sqrt{U_p}, 4\sqrt{U_p}]$ , where  $U_p = E_0^2/(4\omega^2)$  is the ponderomotive energy and  $4\sqrt{U_p} = 3.33$  a.u. Secondly, the ion yield around zero momentum increases, especially for Fig. 1(h). In addition, the double-hump structure in Fig. 1(h) is more symmetric than that in Fig. 1(c). All these features in Figs. 1(f)-1(j) are quantitatively consistent with the experimental results of Ref. [5].

The strong phase dependence of the differential momentum spectra of  $\text{Ar}^{2+}$  ions from NSDI by linearly polarized few-cycle pulses is explained in Ref. [5] using a classical model and Ref. [25] by solving the one-dimensional time-dependent Schrödinger equation (1D TDSE). However, the two models only reproduce the experimental results qualitatively. The calculations of the two models show large deviations in the momentum range and the yield around zero momentum. The classical model in [5] discards the events for the returning electrons with kinetic energy below the ionization potential of the singly charged ion when recollision occurs. Therefore, the distribution around zero momentum is excluded by this classical model. The 1D TDSE gives distribution around zero momentum with yield much higher than the experimental results because of the reduced dimensionality model. Both models give a border momentum range than the experimental results. For multi-cycles pulses, the ion momentum distribution is symmetric since the amplitude of the electric field envelopes of successive half-cycles are the same. While for few-cycle pulses, they changes significantly and depend strongly on the carrier-envelope phase (CEP). This gives rise to asymmetric ion momentum distributions. For some CEP, there are two consecutive half-cycles contributing effectively to NSDI and thus a doublet in the ion momentum distribution may be observed.

Fig. 2 displays the corresponding correlated electron final-state momentum distributions parallel to the laser polarization direction for different CEPs, where the soft-core parameter  $a = 1.5$  a.u. for Figs. 2(a)-2(e) and 1.0 a.u. for Figs. 2(f)-2(j) after first ionization. White boxes indicate  $\pm 2\sqrt{U_p} = \pm 1.66$  a.u. The correlated electron final-state momentum distributions have a strong dependence on the CEP of the few-cycle pulse. The total double ionization yields from the first and third quadrants are much higher than those from the second and fourth quadrants. Furthermore, the double ionization yields from the first and the third quadrants depend strongly on the CEP, while that from the second and the fourth quadrants depend slightly on the CEP.

Double ionization events due to (e, 2e) mechanism can only be found in the first and the third quadrants of the final-state electron-electron longitudinal momentum distributions, while due to RESI mechanism can be found in all quadrants because of the subsequently independent emission of the electrons [18]. Therefore, the shape of final-state the electron-electron momentum distributions in Fig.2 shows that both mechanisms are significant to double ionization. Com-

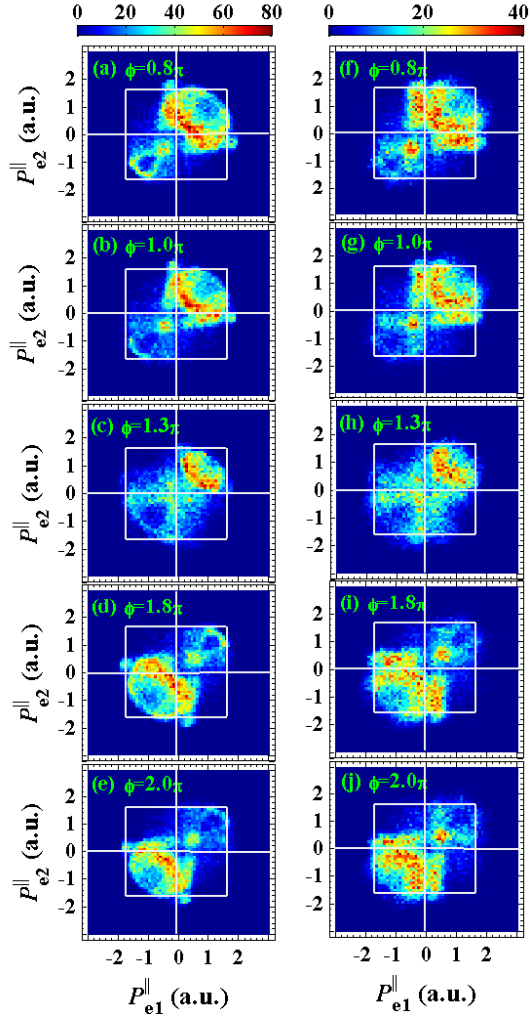


Fig. 2. (color online). Correlated electron momentum distributions parallel to the laser polarization direction of argon NSDI for different CEPs. The laser parameters are the same as Fig. 1. The soft-core parameters  $a = 1.5$  a.u. for Figs. 2(a)-2(e) and 1.0 a.u. for Figs. 2(f)-2(j) after first ionization. White boxes indicate  $\pm 2\sqrt{U_p} = \pm 1.66$  a.u.

paring Figs. 2(f)-2(j) with Figs. 2(a)-2(e) respectively, we can find that double ionization yields from the second and fourth quadrants increases a little when parameter  $a$  decreases from 1.5 to 1 a.u. after first ionization. According to [26], if the delay time between closest recollision and double ionization is less than 0.25 laser cycle, the physical mechanism of double ionization is classified to RCI and the mechanism is RESI if the delay time larger than 0.25 laser cycle. The statistic results show the double ionization yield due to RESI is about 50% when  $a = 1.5$  a.u. after first ionization. While the double ionization yield due to RESI increases to above 60% when  $a = 1$  a.u. after the first ionization. The enhancement of contribution of RESI leads to the ion yield around zero momentum increasing. This is well understandable because the nuclear Coulomb attraction to the electrons becomes larger as parameter  $a$  decreases. As a result, the two electrons are hard to ionized through RCI mechanism. A lower shielding parameter

$a$  implies a more important role of the nuclear Coulomb attraction in recollision. The good agreement between our simulations and the experiments indicates that  $a = 1$  for Ar atoms is the

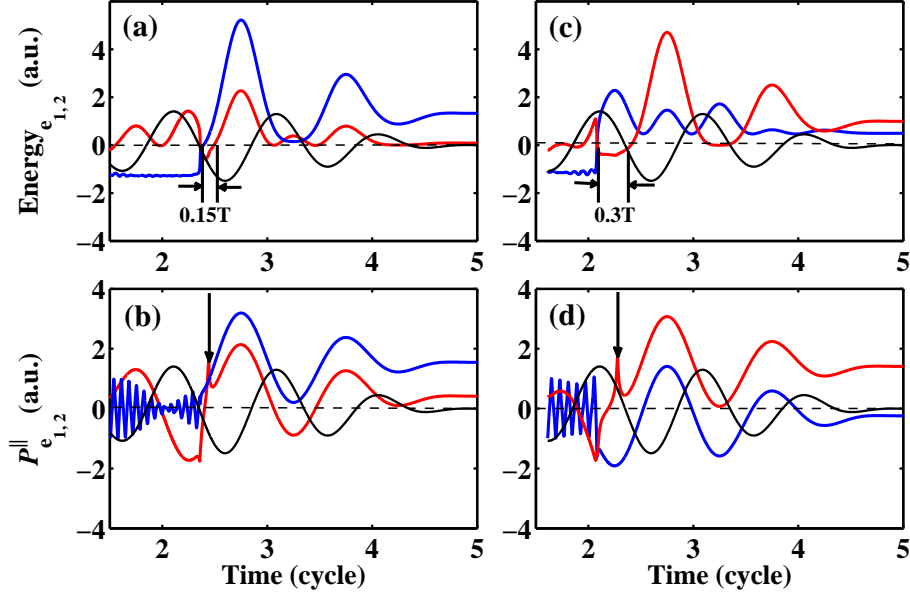


Fig. 3. (color online). Typical trajectories for NSDI: (a) and (c) are energy trajectories. (b) and (d) are momentum trajectories. Where the blue and red curves indicate the first and the second electrons, respectively. The black curve represents the electric field of the laser pulse. (a) and (b) correspond to the electrons from the first quadrant of Fig. 1(f). (c) and (d) correspond to the electrons from the second or fourth quadrant of Fig. 1(f).

In order to explore the influence of nuclear Coulomb potential on the electrons in double ionization process, we take advantage of the back analysis of the classical model. Taking  $\phi=0.8\pi$  as an example, back analysis shows that there are two typical trajectories displayed in Fig. 3. One of the typical trajectories [see Figs. 3(a) and 3(b)] comes from the first quadrant of Fig. 2(f). Firstly, the first electron is field-ionized (the red line) and thus possesses a positive energy. Its energy and momentum is determined by the laser electric field. The second electron is bounded by nucleus (the blue line) and possesses a negative energy. At about 2.35 laser cycles, the momentum of the first electron changes suddenly, decreasing to zero rapidly. This implies that recollision occurs. At the same time, the energy of the second electron rapidly increases and is directly recollision-ionized in a very short time interval. The first electron is firstly bounded and then ionized by the laser electric field. Before ionized, the momentum of the first electron changes suddenly [as indicated by the arrow in Fig. 3(b)], implying that the nucleus imposes a strong attraction of this electron. Finally, the dynamics of both electrons are determined by the laser electric field. This process spends about 0.15 laser cycle. The other typical trajectory [see Figs. 3(c) and 3(d)] comes from the second quadrant of Fig. 2(f). The delay time between recollision and double ionization lasts about 0.3 laser cycle. This trajectory shows the similar behavior [indicated by the arrow in Fig. 3(d)]. The trajectory analysis reveals that the nuclear Coulomb attraction plays an important role in the microscopic dynamics in the

process between recollision and final double ionization.

The above results verifies that the soft-core parameter  $a = 1$  a.u after first ionization is suitable to describe the role of nuclear Coulomb attraction in recollision process of NSDI of Ar atoms. It is confirmed once again by the simulation results of NSDI of Ar atoms with laser intensities below the recollision threshold, which are given below. Therefore, our theoretical simulations provide a reliable benchmark for determining the CEP of the few-cycle pulses by comparing with the experimental results using phase-dependent NSDI. Fig. 4 shows the ratio of total NSDI yields from the first and from the third quadrants as a function of the CEP. The ratio increases rapidly for the CEP ranging from  $0.2\pi$  to  $0.7\pi$  and decreases rapidly for the CE in 1

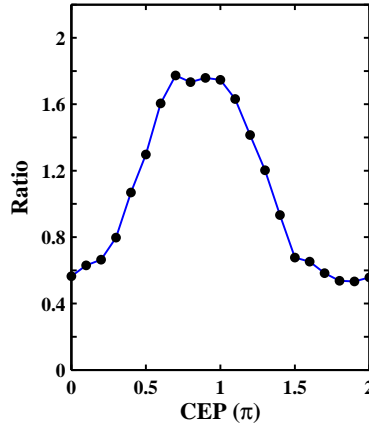


Fig. 4. (color online). Ratio of the total NSDI yields from the first and the third quadrants as a function of the CEP. The all calculated parameters are the same as in Fig. 1. The circles are the calculated data. The solid line is drawn to guide the eye.

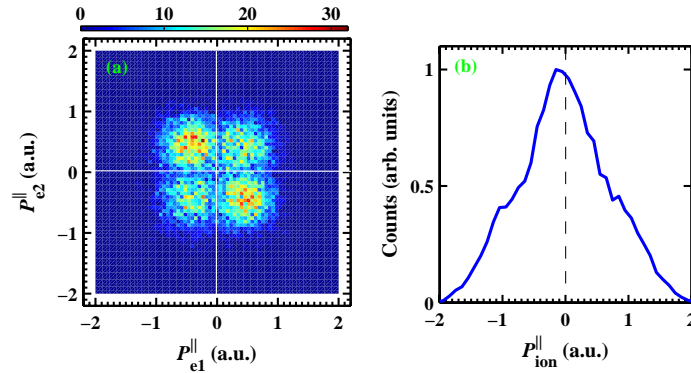


Fig. 5. (color online). (a) Correlated longitudinal momentum distribution  $P_{e1}^{\parallel}$  vs  $P_{e2}^{\parallel}$  for argon double ionization. (b) Longitudinal momentum spectra of  $\text{Ar}^{2+}$  ions. The intensity  $I=0.7 \times 10^{14}$  W/cm<sup>2</sup>.



Finally, we give the simulation results of NSDI of Ar atoms by an intense laser pulse with intensity below the recollision threshold. The pulse is trapezoidal shape with two-cycle turn on, six cycles at full strength and two-cycle turn off. The wavelength  $\lambda=800$  nm and the intensity  $I=0.7\times 10^{14}$  W/cm<sup>2</sup>, are the same as in the experiment of Ref. [10]. Here, the employed ensemble contains two million classical electron pairs. Figs 5(a) and 5(b) show the correlated electron and doubly charged ion longitudinal momentum distributions respectively for  $a = 1$  a.u. after first ionization. Two prominent features are seen in Fig. 5(a): the dominance of events for electron emission into opposite hemispheres and a clear minimum at the origin. The ion longitudinal momentum spectra in Fig. 5(b) shows a sharp maximum around zero momentum, in contrast to the characteristic double-hump structure of NSDI with intensities above the recollision threshold. The resulting correlated momentum distributions in Figs. 5(a) and 5(b) are in excellent agreement with the experimental results in Figs. 2(b) and 2(d) of Ref. [10], respectively. Below the recollision threshold, such perfect agreement once again prove that the value of the soft-core parameters  $a$  selected in this paper accurately describe the nuclear Coulomb attraction in the double ionization process of Ar atoms.

We also analyze the double ionization process for the laser intensity below recollision threshold. Back analysis reveals that the RESI mechanism is the dominant process and most of the trajectories only include one collision. For the trajectories from the first and third quadrants of Fig. 5(a), one electron ionized immediately after recollision while the other electron is excited by recollision and then emits with laser-assisted ionization just before the subsequent peak of the electric field. For the trajectories from the second and fourth quadrants in Fig. 5(a), both electrons are excited by recollision, and then they get ionized step by step around various electric fields [14]. For this intensity, the electrons spend a significant time at the excited states after recollision, where the nuclear Coulomb force is effective. Thus the nuclear Coulomb attraction plays an important role in the ionization process of argon at this laser intensity.

The parameter  $a$  after first ionization for Ar atoms is much different from that for He atoms. Ref. [20] has shown that when the soft-core parameters  $a$  after first ionization is very small ( $\ll 1$  a.u.), the simulation results using the 3D classical ensembles are in good agreement with experimental results [18, 19]. The remarkable difference between the values of  $a$  for He and Ar atoms essentially originates from the different atomic structures. He possesses only two electrons, while Ar possesses eighteen electrons. Except the two outer active electrons, the inner sixteen electrons of Ar exert a shielding effect on the nuclear Coulomb attraction to the two outermost electrons. As a consequence, it leads to suppressed influence of Ar nucleus in NSDI process, compared with the case of He. This implies that the influence of the inner electrons for many-electron atoms plays a significant role in the dynamic details in strong-field double ionization process.

#### 4. Summary

In summary, we have exploited the 3D classical ensembles to investigate the strong-field NSDI of Ar atoms. By adjusting the nuclear Coulomb potential to some proper form after first ionization, we can quantitatively reproduce the experimental correlated electron and doubly charged ion momentum spectra from NSDI of Ar for both laser intensities above and below the recollision threshold. This means that the 3D classical ensembles can provide reliable simulation supports for determining the CEP of few-cycle pulses using NSDI by comparing with experimental measurements. Trajectory analysis reveals a sudden momentum change of one electron, implying that the nuclear Coulomb attraction plays a key role in the microscopic dynamics in process at and after recollision. The significant difference of nuclear Coulomb potentials for He and Ar implies the unignorable influence of the inner electrons of Ar on NSDI.

## **ACKNOWLEDGMENTS**

This work was supported by the National Natural Science Foundation of China under Grant No. 10774054, National Science Fund for Distinguished Young Scholars under Grant No.60925021, and the 973 Program of China under Grant No. 2006CB806006.